Applied Surface Science 274 (2013) 1–6

Contents lists available at SciVerse ScienceDirect

Applied Surface Science

journal homepage: www.elsevier.com/locate/apsusc

Theoretical study on the reactivity of the surface of pure oxides: The Influence of the support and oxygen vacancies

Walter G. Reimers[a], Miguel A. Baltanás[b], María Marta Branda[a,*]

[a] IFISUR (Instituto de Física del Sur) UNS-CONICET, Av. Alem 1253, Bahía Blanca 8000, Argentina
[b] INTEC (Instituto de Desarrollo Tecnológico para la Industria Química) UNL-CONICET, Güemes 3450, Santa Fe S3000GLN, Argentina

ARTICLE INFO

Article history:
Received 15 September 2012
Received in revised form 23 January 2013
Accepted 24 January 2013
Available online 14 March 2013

Keywords:
Pure oxides
Supported oxides
DFT
Reactivity
Adsorption
Gallia
Ceria
Zinc oxide

ABSTRACT

The surface reactivity of three oxides widely used as heterogeneous catalysts, CeO_2 (ceria), Ga_2O_3 (gallia), and ZnO, with CO, CO_2, and H_2 was investigated. The most stable perfect (dehydroxylated) oxide surfaces, surfaces that contain oxygen vacancies, and monolayers of Ga_2O_3 and ZnO epitaxially grown over CeO_2(1 1 1) were investigated using DFT calculations. As expected, CO_2 exhibited the highest adsorption energies on almost every surface. The only observed exceptions were the ZnO surfaces, viz., the ZnO(0 0 0 1) perfect surface and a ZnO monolayer grown on ceria, with which the CO molecule interacts more strongly and generates CO_2 species. In contrast, H_2 interacts weakly with the majority of the surfaces, with the exception of gallia/ceria, where this molecule dissociates. The oxides become considerably more reactive when oxygen vacancies are present on the surface. The reactivity of the CeO_2(1 1 1) and Ga_2O_3(1 0 0) surfaces that contain oxygen vacancies increases up to ten-times with respect to the perfect surfaces. In addition, both Ga_2O_3 and ZnO also exhibit an important increase of their reactivity when they are supported on ceria. Thin films of these oxides that are epitaxially grown onto ceria surfaces have shown to be highly suitable catalysts for oxidizing CO and CO_2 molecules and for dissociating the H_2 molecule.

© 2013 Elsevier B.V. All rights reserved.

1. Introduction

The last UN Climate Change Conferences have confirmed that conventional fossil fuels (petroleum, carbon, and natural gas) will remain as the predominant source of energy used by mankind during this century [1]. These conferences have clearly indicated that the atmospheric accumulation of CO_2 and the consequent greenhouse effect are crucial issues that require immediate action. In this respect, the signing countries have pledged to reduce CO_2 emissions and to search for new alternatives to mitigate the impacts from the combustion of fuels.

The capturing and recycling of CO_2 via chemical processes to create to carbon-neutral liquid fuel derivatives or hydrogen vectors, such as methanol and dimethyl ether, has now become a viable alternative [2,3]. Methanol reforming is particularly suitable for supplying this ubiquitous feedstock to fuel cells [4].

These processes demand novel, multifunctional catalytic materials. Precious metals supported on medium to high-surface area oxides (with or without added promoters) remain the preferred choices. To synthesize methanol from carbon oxides, such as CO and/or CO_2, Baltanás and co-workers developed ultradisperse Pd/silica-promoted catalysts capable of hydrogenating CO/H_2 (Ca–Pd/silica) or CO_2/H_2 (Ga–Pd/silica) mixtures [5–8]. These developments followed the finding by Fujitani et al. that palladium deposited on gallium oxide (Pd/Ga_2O_3) was 20 times more active for producing methanol from CO_2/H_2 than the traditional Cu/ZnO catalyst [9]. Indeed, the actual role of Ga_2O_3 (usually known as 'gallia', which is a reducible oxide) in the process subsequently became of the utmost interest [10].

Likewise, the excellent properties of CeO_2 (common name 'ceria') for transporting oxygen and its redox ability to easily interchange between the Ce^{4+} and Ce^{3+} oxidation states have been known for several decades [11,12]. Ceria is currently used in several electronic applications, such as gate dielectrics and photovoltaic cells [13,14], and it is used as a component of ion conducting films in fuel cells [15]. Ceria is also recognized as a versatile material in modern heterogeneous catalysis, notably as a key component of the three-way catalysts (TWCs), in which this oxide has proven to be highly effective for the conversion of noxious car exhaust gases [16]. The epitaxial coverage of ceria with gallia, for instance, could lead to novel catalytic materials that have unique selectivity and/or activity in processes where carbon oxides are involved.

Considering that the generation of methanol from CO, CO_2 and H_2 molecules first requires the adsorption of the molecule(s) onto

* Corresponding author. Tel.: +54 291 4595101.
E-mail address: cabranda@criba.edu.ar (M.M. Branda).

0169-4332/$ – see front matter © 2013 Elsevier B.V. All rights reserved.
http://dx.doi.org/10.1016/j.apsusc.2013.01.177

the surface of the catalyst, we have performed a systematic analysis of the interactions of these molecules with different ceria, gallia and ZnO surfaces. Specifically, with the objective of obtaining a broad database to gain in-depth knowledge about the surface adsorptive properties of these materials, we have focused on the molecular interactions of these gaseous reactants with the CeO_2(1 1 1), CeO_2(3 3 1), Ga_2O_3(1 0 0) and ZnO(0 0 0 1) dehydroxylated surfaces that exhibit the most stable faces [17,18] using DFT calculations. The influence of surface oxygen vacancies on the reactivity and the interaction of the same molecules on epitaxial grown gallium and zinc oxides on the CeO_2(1 1 1) surface were also investigated.

2. Computational details

Self-consistent density functional theory (DFT) calculations using periodic slab models were conducted to investigate the adsorption of CO, H_2 and CO_2 molecules onto the regular surfaces of CeO_2(1 1 1), CeO_2(3 3 1), Ga_2O_3(1 0 0) and ZnO(0 0 0 1). The surfaces of ceria and gallia that contained an oxygen vacancy, which are subsequently designated as CeO_2(1 1 1) vacO and Ga_2O_3(1 0 0) vacO, respectively, were also investigated. The calculations were performed using the VASP code [19,20], in which one-electron wavefunctions are expanded on the basis of periodic plane-waves.

The PAW method [21,22] was used to represent the inner cores, and one electron states were expanded on a plane-wave basis. The kinetic energy cutoff and *k*-point grid values were chosen after a systematic study of the geometries and energy convergence with the *k*-points grid and cutoff energies for the adsorptions of CO, CO_2 and H_2 onto every investigated surface. These test calculations revealed that a kinetic cut-off energy of 415 eV was sufficient to achieve convergence for all the calculations performed in this work. Different Monkhorst–Pack grids of special *k*-points were employed for every case [23].

Both the local density approximation of the Vosko–Wilk–Nusair (VWN) type [24] and the PW91 [25,26] form of the generalized gradient approximation were employed. Because both the local density (LDA) and generalized gradient (GGA) approximations fail to describe the strong localization of the *4f* electrons of Ce^{3+}, all the calculations on ceria were performed using the LDA + *U* and GGA + *U* approaches. In these cases, the Hubbard parameter (*U*) penalizes the double occupation of the *4f* orbital [27,28].

The mentioned failure of DFT also could be overcome by employing hybrid functionals. Hybrid density functional calculations on CeO_2 and Ce_2O_3 led to an accurate description of both systems [29,30], but present a lot of computational problems. Among others, these calculations carried out on relatively small unit cells of slab models are computationally expensive [31,32]. A way of avoiding these difficulties is the use of LDA and GGA exchange-correlated potentials correcting the self-interaction error by means of a Hubbard-like term by explicit inclusion of an effective local two-electron one-center repulsion term, *U* [27,33,34]. The selection of *U* is not easy and the best value may depend on the studied properties, and the optimum *U* values for LDA and GGA can be different [35]. Loschen et al. have found that for GGA + *U* calculations a value of *U* = 3 eV provides a balanced description of CeO_2 and Ce_2O_3 while for LDA + *U* calculations a larger value of *U* = 5 eV is recommended instead [36]. Besides, for simple oxides and metals, both LDA and GGA predict lattice parameters very close to the experimental data. However, for more complex oxides or for transition metals involving heavy atoms, GGA overestimates interatomic distances; whereas LDA predicts values that are still close to experiment. In recent studies of stepped ceria surfaces [37], ceria nanoparticles [38–40], and the adsorption of Au on ceria [41], some of us suggested using the LDA + *U* (*U* = 5 eV) geometry while employing GGA + *U* (*U* = 3 eV) to obtain the energy and the electron density. This option could present difficulties in the calculation of properties where the stress plays an important role. In addition, the employment of different approaches to the calculation of geometry and electronic properties also could be problematic in systems where they are highly related. Taking into account that the goal of this work is the study of the influence that the oxygen vacancies and the support could have on the surface reactivity and not to discuss the better methodology choice, LDA + *U* (*U* = 5 eV) was used to perform the geometric optimization and then single-point calculations using GGA + *U* (*U* = 3 eV) were performed to obtain the electronic properties of the systems.

Slab models simulate the surface from a unit cell of the atom set with periodical conditions. The size of this cell depends on the size and shape of the molecule to be adsorbed and on the surface coverage to be studied.

Periodic boundary conditions imposed on the electrostatic potential of an asymmetric slab could give rise to an artificial electric field across the slab. Therefore, because the slabs analyzed in this work are not symmetric, we conducted single-point calculations using the dipole correction to analyze possible changes in the adsorption energy values [42,43].

The total energy tolerance defining the self-consistency of the electron density was 10^{-4} eV. The structures were optimized until the maximum forces acting on each atom became less than 0.01 eV/Å.

The perfect surface of CeO_2(1 1 1) and the one that contained oxygen vacancies were represented by slabs (2×2) with nine atomic layers. The perfect surface of CeO_2(3 3 1) was represented by slabs (2×1) with 18 atomic layers. Stoichiometric slabs (2×2) of Ga_2O_3(1 0 0) and ZnO(0 0 0 1) with ten and eight atomic layers, respectively, were used to simulate the perfect surfaces and the surface that contained oxygen vacancies of gallia. Finally, slabs with one layer of Ga_2O_3 and ZnO over the slab of CeO_2(1 1 1) were constructed to represent gallia and ZnO epitaxially grown onto ceria. These mono-layers of Ga_2O_3 and ZnO together with the top ceria layer were fully relaxed. All the slab models were separated by more than 10 Å vacuum widths.

For the geometrical optimization, the joint relaxation of the CO, CO_2 and H_2 molecules and the top layers of the oxides was allowed.

3. Results and discussion

3.1. Reactivity of CeO_2(1 1 1) and CeO_2(331); Ga_2O_3(100) and ZnO(0 0 0 1) perfect surfaces

The energies for the adsorption of CO, CO_2 and H_2 onto each of the surfaces investigated in this work are shown in Table 1. The calculated energy values for the adsorption of CO onto almost every surface without defects are very small, with the only exception of ZnO(0 0 0 1). For the latter case, the energy value is −1.96 eV using the LDA approach and −1.28 eV using the GGA approach. This large adsorption energy can be attributed to the formation of a CO_2 molecule due to the reaction of CO with a surface oxygen atom (see Fig. 1).

Table 2 presents the Voronoi atomic charges for each atom of the molecules after the adsorption process. On the ceria and gallia surfaces, the CO interaction is only electrostatic, and this interaction changes the charge polarity from that of the free CO; the C atom becomes positive and the O atom becomes negative. The CO molecule adopts a negative charge, and this charge is placed on the O atom (see Table 2). However, when the adsorption of CO occurs on ZnO, the charges corresponding to the formed CO_2 tend to be similar to the ones on the CO_2 free molecule (see the atomic charge values at the bottom of Table 2).

Table 1
Adsorption energies (eV) of CO, CO_2, and H_2, calculated using the LDA and GGA (in brackets) approaches for all the investigated surfaces. CeO_2(1 1 1) vacO and Ga_2O_3(1 0 0) vacO represent the ceria and gallia surfaces that contain oxygen vacancies, respectively.

	E_{ads}(CO)	E_{ads}(CO_2)	E_{ads}(H_2)
CeO_2(1 1 1)	−0.21 (+0.11)	−1.20 (−0.37)	−0.05 (+0.01)
CeO_2(3 3 1)	−0.44 (+0.34)	−1.18 (−0.45)	−0.13 (−0.07)
Ga_2O_3(1 0 0)	−0.09 (+0.31)	−0.30 (+0.45)	−0.10 (+0.08)
ZnO(0 0 0 1)	−1.96 (−1.28)	−0.09 (+0.44)	−0.05 (+0.06)
CeO_2(1 1 1) vacO	−0.91 (−0.27)	−1.85 (−0.91)	−0.31 (−0.09)
Ga_2O_3(1 0 0) vacO	−0.92 (−0.18)	−0.97 (−0.50)	−0.90 (−0.02)
Ga_2O_3/CeO_2(1 1 1)	−0.25 (+0.16)	−0.99 (−0.52)	−1.43 (−1.28)
ZnO/CeO_2(1 1;1)	−4.05 (−5.51)	−0.65 (+0.99)	+0.05 (+0.27)

$E_{ads} = E$(molecule/surface) − E(free molecule) − E(surface)

Table 2
Voronoi atomic charges of CO, CO_2 and H_2 adsorbed onto the indicated surfaces. CeO_2(1 1 1) vacO and Ga_2O_3(1 0 0) vacO represent the ceria and gallia surfaces that contain oxygen vacancies, respectively. The charge units are in u.a.

	Q_C (CO)	Q_H (CO)	Q_C (CO_2)	Q_O (CO_2)	Q_H (H_2)
CeO_2(1 1 1)	+0.18	−0.19	+0.42	−0.51/−0.61	0.00/−0.12
CeO_2(3 3 1)	+0.04	−0.36	+0.57	−0.47/−0.73	0.00/0.00
Ga_2O_3(1 0 0)	+0.02	−0.23	+0.46	−0.21/−0.33	−0.10/−0.02
ZnO(0 0 0 1)	+0.66	−0.20	+0.39	−0.38/−0.38	−0.19/−0.04
CeO_2(1 1 1) vacO	−0.49	−0.25	−0.11	−0.62/−0.56	−0.48/−0.15
Ga_2O_3(1 0 0) vacO	−0.17	−0.33	+0.22	−0.42/−0.64	−0.56/−0.72
Ga_2O_3/CeO_2(1 1 1)	+0.18	−0.44	+0.46	−0.26/−0.45	−0.12/−0.05
ZnO/CeO_2(1 1 1)	+0.51	−0.02	+0.62	−0.20/−0.21	−0.02/+0.09

Q_C (CO free) = −0.03, Q_O (CO free) = +0.03, Q_C (CO_2 free) = +0.78, Q_O (CO_2 free) = −0.39, Q_H (H_2 free) = 0.00

The interaction of CO_2 with the perfect oxide surfaces is considerably stronger than the one found with the CO molecule. The exception is, again, that corresponding to the ZnO surface, where the molecule does not adsorb (see Table 1).

For every studied ceria face, the molecule reacts to form $CO_3^=$ species with adsorption energies of −1.20 eV (see Table 1 and Fig. 2). Comparing the atomic charges of the adsorbed CO_2 on the perfect surfaces of ceria with the ones of the free molecule, an important negative charge transference from the surfaces is detected (see Table 2).

However, the gallia surface is weakly reactive in front of CO_2, with an adsorption energy of −0.3 eV (LDA approach). This interaction is only electrostatic, and the adsorbed molecule maintains the original structure of the free one. No charge transfer is observed in this case (see Table 2).

On ZnO, the reactivity toward CO_2 is almost negligible, and only the carbon atom adopts some negative charge (see Tables 1 and 2).

Lastly, H_2 does not react on any of the perfect surfaces (see Table 1). This molecule only exhibits a weak physical interaction with such surfaces, exhibiting a very small electronic charge transfer from the substrate (see Table 2).

The dipole correction does not have an appreciable effect on the adsorption energy values. The observed differences were in the third decimal digit for the molecular adsorptions onto CeO_2(1 1 1), CeO_2(3 3 1) and Ga_2O_3(1 0 0). Only the adsorption of CO_2 onto ZnO(0 0 0 1) was modified, and the adsorption energy changed from −0.09 eV to +0.33 eV. This energy change due to the dipole correction is not small, but the conclusions are the same; the ZnO(0 0 0 1) surface is not reactive toward the CO_2 molecule.

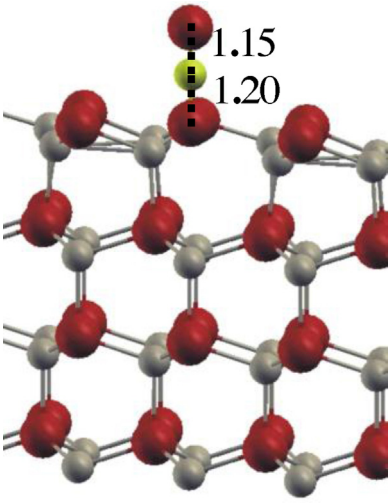

Fig. 1. Adsorption of CO onto the perfect ZnO(0 0 0 1) surface. Grey spheres: Zn atoms, red spheres: O atoms, and yellow spheres: C atoms. Interatomic distances are in Å. (For interpretation of the references to color in this figure legend, the reader is referred to the web version of the article.)

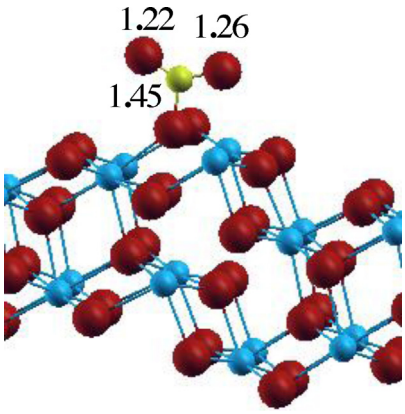

Fig. 2. Adsorption of CO_2 onto the perfect CeO_2(3 3 1) surface. Blue spheres: Ce atoms, red spheres: O atoms, and yellow spheres: C atoms. Interatomic distances are in Å. (For interpretation of the references to color in this figure legend, the reader is referred to the web version of the article.)

Table 3
Voronoi atomic charges calculated for the surface cations of the investigated surfaces. In the cases where there is more than one oxidation state, only the charge of the reduced cation is shown. The charge units are in u.a.

Oxide	Surface cation
CeO_2(1 1 1)	+2.97
CeO_2(3 3 1)	+2.93
Ga_2O_3(1 0 0)	+1.55
ZnO(0 0 0 1)	+1.17
CeO_2(1 1 1) vacO	+2.64
Ga_2O_3(1 0 0) vacO	+0.97
Ga_2O_3/CeO_2(1 1 1)	+1.22
ZnO/CeO_2(1 1 1)	+0.68

3.2. Reactivity of the CeO_2(1 1 1) and Ga_2O_3(1 0 0) surfaces that contain oxygen vacancies (vacO)

The calculated Voronoi atomic charges for the surface cations on all the investigated surfaces are presented in Table 3. The generation of an oxygen vacancy on the CeO_2 surface should result in the reduction of two Ce ions, from Ce^{4+} to Ce^{3+}. The present calculations reveal the reduction of the Ce atom close to the O vacancy from Ce^{4+} (Voronoi charge: +2.97 e) to Ce^{3+} (Voronoi charge: +2.64 e), but the other electron is delocalized on three Ce surface atoms with Voronoi charges of approximately +2.9 e. This electronic delocalization was partially corrected with the use of the Hubbard parameter (U) in the DFT calculations, but the electronic localization was not complete [27]. However, we have chosen the site near the Ce^{3+} ion to adsorb the molecules.

Noteworthy, the oxygen vacancy on the gallia surface results in the reduction of an adjacent Ga^{3+} ion (Voronoi charge: +1.55 e) to Ga^{1+} (Voronoi charge: +0.97 e), as observed in Table 3.

The adsorptions of CO and CO_2 onto the oxide surfaces that have oxygen vacancies are both significantly stronger than the ones onto the perfect surfaces (see the E_{ads} values in Table 1). The CO molecule adsorbs with the C atom that occupies the location of the vacancy on both surfaces. Fig. 3 shows the adsorption of CO onto ceria (1 1 1) vacO. Conversely, the most stable geometric configuration for CO_2 on both investigated surfaces that contains oxygen vacancies is that where the oxygen atom occupies the vacancy location (see Fig. 4). Both molecules, CO and CO_2, take electronic charge from the surfaces (see Table 2). The surface atom of ceria vacO that transfers charge to the CO_2 molecule is the Ce^{3+} ion, which is oxidized to Ce^{4+}. In the case of gallia vacO, the charge transfer to the molecule occurs from the Ga^{1+} ion, which is oxidized to Ga^{3+} (see Table 2).

The H_2 molecule also interacts more strongly with the oxygen deficient surfaces (see adsorption energies in Table 1). An important charge transfer from the oxide surfaces to the molecule is observed, and it is considerably greater on gallia vacO than on ceria vacO (see Table 2). These charge transfers also involve

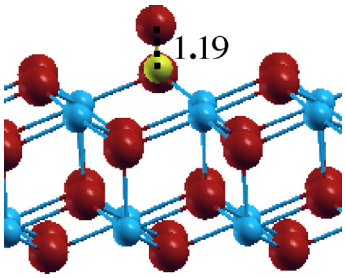

Fig. 3. Adsorption of CO onto the CeO_2(1 1 1) surface that contains oxygen vacancies (designated as CeO_2(1 1 1) vacO in the text). Blue spheres: Ce atoms, red spheres: O atoms, and yellow spheres: C atoms. Interatomic distances are in Å. (For interpretation of the references to color in this figure legend, the reader is referred to the web version of the article.)

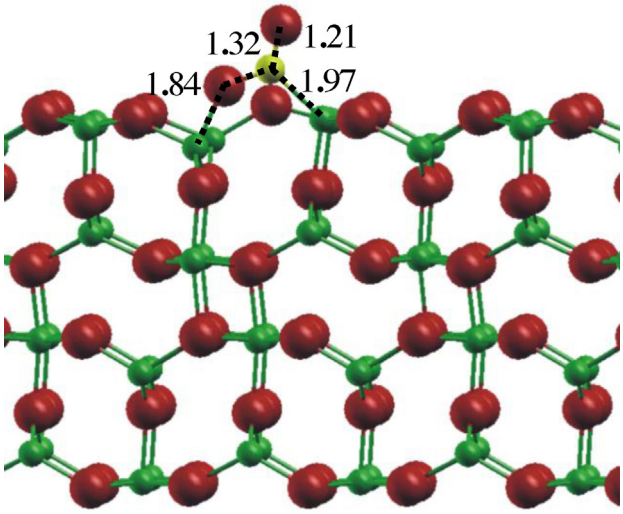

Fig. 4. Adsorption of CO_2 onto the Ga_2O_3(1 0 0) surface that contains oxygen vacancies (designated as Ga_2O_3(1 0 0) vacO in the text). Green spheres: Ga atoms, red spheres: O atoms, and yellow spheres: C atoms. Interatomic distances are in Å. (For interpretation of the references to color in this figure legend, the reader is referred to the web version of the article.)

the oxidation of surface Ga^{1+} and Ce^{3+} ions, respectively. The adsorption of H_2 onto the Gallia vacO surface is associated with the spontaneous dissociation of the molecule (see Fig. 5).

Contrary to our expectations, the dipole correction performed during the calculations of the adsorption energy values for the surfaces that contained oxygen vacancies did not have an appreciable effect. The energy values only changed by hundredths of an eV.

3.3. Reactivity of Ga_2O_3 and ZnO and monolayers epitaxially grown over CeO_2(1 1 1)

The obtained energies for the adsorption of the three investigated molecules onto the Ga_2O_3 and ZnO and monolayers are significantly greater than those for their adsorptions onto the perfect surfaces (see Table 1). Similar to the surfaces that contain oxygen vacancies, this significant reactivity can be attributed to the presence of reduced cations on the surface (see Table 3).

The CO molecule adsorbs onto the supported monolayers with adsorption energies that are three-times (Ga_2O_3/CeO_2) or

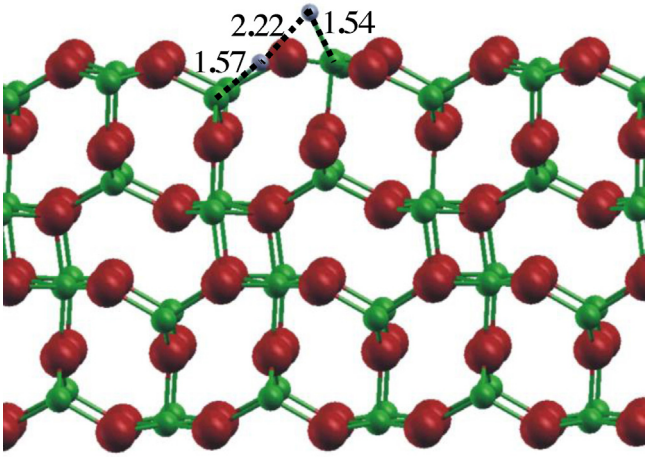

Fig. 5. Adsorption of H_2 onto the Ga_2O_3(1 0 0) vacO surface. Green spheres: Ga atoms, red spheres: O atoms, and white spheres: H atoms. Interatomic distances are in Å. (For interpretation of the references to color in this figure legend, the reader is referred to the web version of the article.)

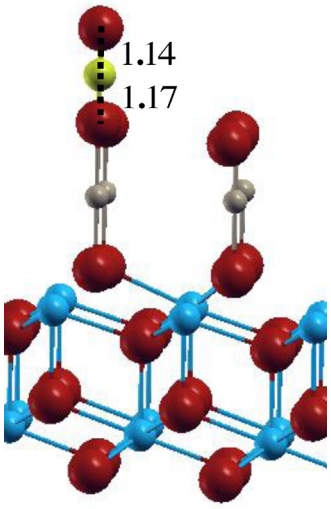

Fig. 6. Adsorption of CO onto the $ZnO/CeO_2(1\,1\,1)$ surface. Grey spheres: Zn atoms, blue spheres: Ce atoms, red spheres: O atoms, and yellow spheres: C atoms. Interatomic distances are in Å. (For interpretation of the references to color in this figure legend, the reader is referred to the web version of the article.)

two-times (ZnO/CeO_2) greater than those corresponding to the perfect Ga_2O_3 and ZnO surfaces, respectively, and in these cases, CO_2 is also formed with the surface oxygen ion (see Fig. 6). Remarkably, the adsorption of the CO_2 molecule onto the epitaxially grown monolayers is between three- and six-times greater than onto the pure oxides. As noted above, the H_2 molecule does not interact with the perfect oxide surfaces, and it weakly reacts on the surfaces that contain oxygen vacancies. The gallia monolayer that was epitaxially grown onto the $CeO_2(1\,1\,1)$ surface is considerably more reactive toward hydrogen and results in the spontaneous dissociation of the molecule (see Fig. 7) with an adsorption energy of 1.43 eV. However, the ZnO monolayer over ceria is unreactive to H_2.

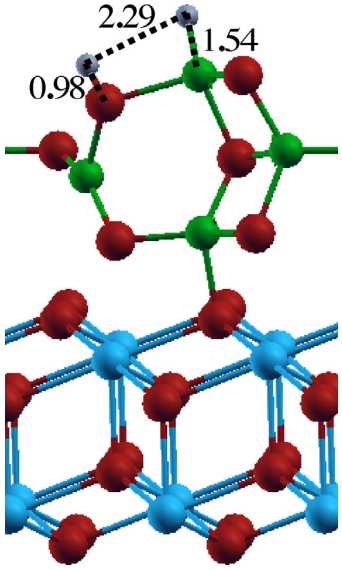

Fig. 7. Adsorption of H_2 onto the $Ga_2O_3/CeO_2(1\,1\,1)$ surface. Green spheres: Ga atoms, blue spheres: Ce atoms, red spheres: O atoms, and white spheres: H atoms. Interatomic distances are in Å. (For interpretation of the references to color in this figure legend, the reader is referred to the web version of the article.)

4. Conclusions

The reactivity with CO, CO_2 and H_2 on two perfect, and more stable ceria surfaces, (1 1 1) and (3 3 1), and on the gallia (1 0 0) and ZnO(0 0 0 1) surfaces was investigated using DFT calculations. The influence of surface oxygen vacancies in the ceria and gallia surfaces on the reactivity was also analyzed. Finally, the effect of the substrate on the oxide reactivity was investigated by examining monolayers of Ga_2O_3 and ZnO that were epitaxially grown over $CeO_2(1\,1\,1)$. The DFT + *U* method was employed to correct the on-site Coulomb correlation and exchange interactions that resulted from the strongly localized Ce-4*f* electrons. The relative ordering of the molecular reactivities with these surfaces was determined to be $CO_2 > CO > H_2$, with the exception of the ZnO(0 0 0 1) and $ZnO/CeO_2(1\,1\,1)$ surfaces, where CO reacts strongly to form CO_2 species. The H_2 molecule was also observed to weakly interact with the majority of the surfaces, with the exception of $Ga_2O_3(1\,0\,0)$ vacO and with the (monolayer) gallia film grown on ceria, where this molecule spontaneously dissociates. In general, these oxide surfaces become considerably more reactive when oxygen vacancies are present. Likewise, both Ga_2O_3 and ZnO also exhibit an important increase of their reactivity when they are supported on ceria. The results indicate that thin films of these oxides epitaxially grown onto ceria surfaces are highly suitable catalysts for oxidizing the CO and CO_2 molecules and for dissociating the H_2 molecule. We believe that the reason for the greater interaction with the investigated molecules is primarily due to the presence of reduced cations on the surfaces of both the oxide surfaces with oxygen vacancies and the thin films on ceria(1 1 1).

References

[1] United Nations Framework Convention on Climate Change, www.unfcc.int
[2] G.A. Olah, A. Goeppert, G.K. Surya Prakash, The Journal of Organic Chemistry 74 (2009) 487–498.
[3] J. Vancoillie, J. Demuynck, L. Sileghem, M. Van De Ginste, S. Verhelst, International Journal of Hydrogen Energy 37 (12) (2012) 9914–9924.
[4] D.R. Palo, R.A. Dagle, J.D. Holladay, Chemical Reviews 107 (2007) 3992–4021.
[5] A.L. Bonivardi, D.L. Chiavassa, M.A. Baltanás, Studies in Surface Science and Catalysis 114 (1998) 533–536.
[6] A.L. Bonivardi, D.L. Chiavassa, C.A. Querini, M.A. Baltanás, Studies in Surface Science and Catalysis 130 (2000) 3747–3752.
[7] S.E. Collins, M.A. Baltanás, J.L. García Fierro, A.L. Bonivardi, Journal of Catalysis 211 (2002) 252–264.
[8] S.E. Collins, M.A. Baltanás, A.L. Bonivardi, Journal of Catalysis 226 (2) (2004) 410–421.
[9] T. Fujitani, M. Saito, Y. Kanai, T. Watanabe, J. Nakamura, T. Uchijima, Applied Catalysis A: General 125 (1995) L199–L202.
[10] D.L. Chiavassa, S.E. Collins, A.L. Bonivardi, M.A. Baltanás, Chemical Engineering Journal 150 (2009) 204–212.
[11] H.C. Yao, Y.F.C. Yao, Journal of Catalysis 86 (1984) 254–260.
[12] K.C. Taylor, Catalysis in catalytic converters, in: J.R. Anderson, M. Boudart (Eds.), Catalysis Science and Technology, vol. 5, Springer, Berlin, 1984, pp. 119–170.
[13] J.-H. Yoo, S.-W. Nam, S.-K. Kang, Y.-H. Jeong, D.-H. Ko, J.-H. Ku, H.-J. Lee, Microelectronic Engineering 56 (1–2) (2001) 187–190.
[14] A. Corma, P. Atienzar, H. García, J.-Y. Chane-Ching, Nature Materials 3 (2004) 394–397.
[15] J. Qiao, K. Sun, N. Zhang, B. Sun, J. Kong, D. Zhou, Journal of Power Sources 169 (2) (2007) 253–258.
[16] A. Trovarelli, C. De Leitenburg, M. Boaro, G. Dolcetti, Catalysis Today 50 (1999) 353–367.
[17] M.M. Branda, R.M. Ferullo, M. Causá, F. Illas, Journal of Physical Chemistry C 115 (2011) 3716–3721.
[18] D. Kohl, Th. Ochs, W. Geyer, M. Fleischer, H. Meixner, Sensors and Actuators B 59 (1999) 140–145.
[19] G. Kresse, J. Furthmuller, Physical Review B 54 (1996) 11169–11186.
[20] G. Kresse, J. Hafner, Physical Review B 47 (1993) 558–561.
[21] G. Kresse, D. Joubert, Physical Review B 59 (1999) 1758–1775.
[22] P.E. Blöchl, Physical Review B 50 (1994) 17953–17979.
[23] H.J. Monkhorst, J.D. Pack, Physical Review B 13 (1976) 5188–5192.
[24] S.H. Vosko, L. Wilk, M. Nusair, Canadian Journal of Physics 58 (1980) 1200–1211.
[25] J.P. Perdew, J.A. Chevary, S.H. Vosko, K.A. Jackson, M.R. Pederson, D.J. Singh, C. Fiolhais, Physical Review B 46 (1992) 6671–6687.
[26] J.P. Perdew, J.A. Chevary, S.H. Vosko, K.A. Jackson, M.R. Pederson, D.J. Singh, C. Fiolhais, Physical Review B 48 (1993) 4978.

[27] V.I. Anisimov, F. Aryasetiawan, A.I. Lichtenstein, Journal of Physics: Condensed Matter 9 (1997) 767–808.
[28] S.L. Dudarev, G.A. Botton, S.Y. Savrasov, C.J. Humphreys, A.P. Sutton, Physical Review B 57 (1998) 1505–1509.
[29] J.L.F. Da Silva, M.V. Ganduglia-Pirovano, J. Sauer, V. Bayer, G. Kresse, Physical Review B 75 (2007) 045121.
[30] P.J. Hay, R.L. Martin, J. Uddin, G.E. Scuseria, Journal of Chemical Physics 125 (2006) 03471.
[31] M.V. Ganduglia-Pirovano, J.L.F. da Silva, J. Sauer, Physical Review Letters 102 (2009) 026101.
[32] C. Franchini, R. Podloucky, F. Allegretti, F. Li, G. Parteder, S. Surnev, F.P. Netzer, Physical Review B 79 (2009) 035420.
[33] V.I. Anisimov, I.V. Solovyev, M.A. Korotin, M.T. Czyzyk, G.A. Sawatzky, Physical Review B 48 (1993) 16929–16934.
[34] I.V. Solovyev, P.H. Dederichs, V.I. Anisimov, Physical Review B 50 (1994) 16861–16871.
[35] C.W.M. Castleton, J. Kullgren, K. Hermansson, Journal of Chemical Physics 127 (244704) (2007) 1–11.
[36] C. Loschen, J. Carrasco, K.M. Neyman, F. Illas, Physical Review B 75 (2007) 035115.
[37] M.M. Branda, C. Loschen, K.M. Neyman, F. Illas, Journal of Physical Chemistry C 112 (2008) 17643–17651.
[38] C. Loschen, S.T. Bromley, K.M. Neyman, F. Illas, Journal of Physical Chemistry C 111 (2007) 10142–10145.
[39] C. Loschen, A. Migani, S.T. Bromley, F. Illas, K.M. Neyman, Physical Chemistry Chemical Physics 10 (2008) 5730–5738.
[40] A. Migani, C. Loschen, F. Illas, K.M. Neyman, Chemical Physics Letters 465 (2008) 106–109.
[41] N.J. Castellani, M.M. Branda, K.M. Neyman, F. Illas, Journal of Physical Chemistry C 113 (2009) 4948–4954.
[42] J. Neugebauer, M. Scheffler, Physical Review B 46 (1992) 16067–16080.
[43] G. Makov, M.C. Payne, Physical Review B 51 (1995) 4014–4022.